

# THE 4TH INTERNATIONAL CONFERENCE ON ALUMINUM ALLOYS

## MICROSTRUCTURE & TEXTURE IN HOT-ROLLED AA1350 ALLOY

Rajeev G. Kamat, Armand J. Beaudoin, Sheila A. Rosenfield & Richard E. Hughes

Reynolds Metals Company  
Corporate Research & Development  
P. O. Box 27003  
Richmond, VA 23261, USA

### Abstract

Aluminum alloy AA1350 was hot-rolled to simulate industrial practice and samples were subjected to microstructural and textural analysis. With increasing reductions a refinement of the subgrain size was observed. Twisting of the sample during the 4th hot-rolling pass was attributed to localized softening, resulting in localized deformation across the sample. This was confirmed by hardness differences across the sample. The edge-to-edge difference in hardness was highest after the 3rd pass.

### Introduction

Aluminum alloys for electrical applications have gained acceptance due to the economic advantages offered by the high speed thermomechanical processing of continuously cast bars into rods. Subsequently these rods are cold-drawn into wires of various diameters depending on the applications. An optimum combination of conductivity, formability, creep resistance and thermal stability is derived by carefully controlling the processing steps from casting to wire-drawing. In this study, the hot-rolling of EC (electrical conductor) grade aluminum alloy AA1350 and the resulting microstructural evolution has been examined.

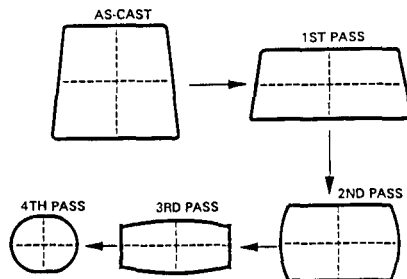


Figure 1: Schematic illustration of typical hot-rolling reductions applied in industrial production of rods.

Figure 1 shows a schematic illustration of the typical hot-rolling reductions applied in the industrial production of rods. Hardness measurements around the periphery and center of the samples after each rolling pass show (Figure 2) an increase in hardness through the first two passes.

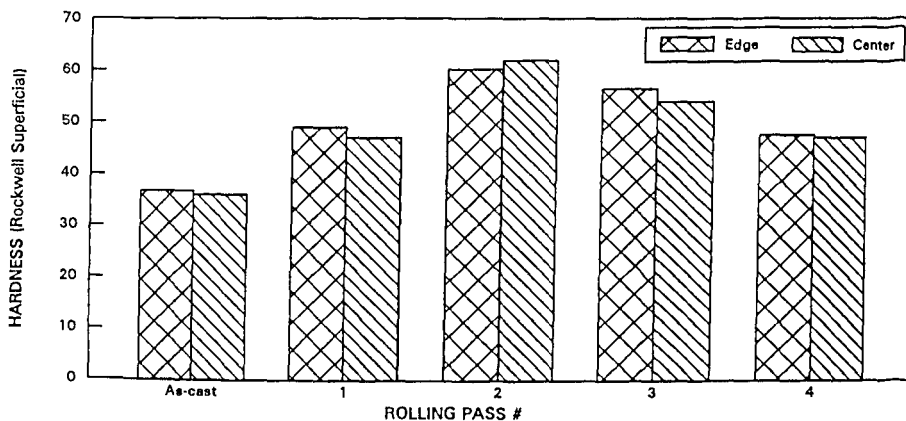


Figure 2: Average hardness measured in the cross-sections perpendicular to the rolling direction in the industrially hot-rolled rods.

This work hardening was similar in the edges as well as the center. Softening was observed in subsequent passes. This is usually related to recovery and/or recrystallization that occurs either between the stands (static) or in the roll-bite (dynamic) at high temperatures and/or high strains. However, for pure aluminum, which has a high stacking fault energy, the consensus is that dynamic recovery is more likely than dynamic recrystallization [1].

In this study an experimental procedure was developed to simulate the industrial hot-rolling process. The main objective of the experimental procedure was to replicate the softening behavior observed in industrial practice. However, a shape instability was observed during hot-rolling and related to a through-the-thickness microstructural variation.

### Materials & Experimental Procedure

The composition of the alloy used in this study is shown in Table 1. This alloy was cast into bars on an industrial scale using a continuous caster.

Table 1: Composition of the alloy used in the study.

Si 0.05	Fe 0.15	Cu 0.001	Mn 0.001	Mg 0.001	Cr 0.001	Ni 0.01	Zn 0.01	Ti 0.001	B 0.005	V 0.001
------------	------------	-------------	-------------	-------------	-------------	------------	------------	-------------	------------	------------

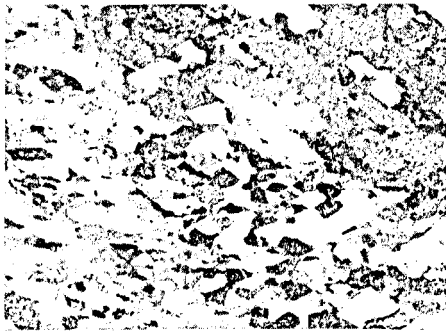
The industrial rolling simulations were carried out on a two-high laboratory reversing mill with internal resistance heating of the work rolls and a recirculating cooling system. The mill is preheated prior to rolling. A stable work roll temperature was achieved through simultaneous use of the internal heating units and coolant sprays. Samples of 2.5 cm x 2.5 cm were machined from the industrially cast bars. Rolling of the as-cast bars on the industrial scale involves a sequence of passes to reduce the cross-section in both the vertical and horizontal dimensions (Figure 1). To simulate the industrial hot-rolling schedule, the bars were turned by 90° after every pass. A number of bar samples were preheated to temperatures of 400° C and 450° C and rolled in four passes. Reductions of 25%, 31%, 24%, and 25% were employed. Samples were quenched in ice water within 5 seconds after each pass for microstructure and hardness measurements.

For macro metallography, samples were etched in a solution consisting of 33% water, 33% HCl, 33% HNO<sub>3</sub> and 1% HF by volume at 55° C for ≈ 1 min. Samples were also electrochemically polished with a perchloric-acid-based solution to enable imaging of the substructure using back-scattered electron channelling contrast (ECC) on the SEM. For optimum results under back-scattered electron imaging, a voltage of 10kV and a working distance of ≈ 12 mm was employed.

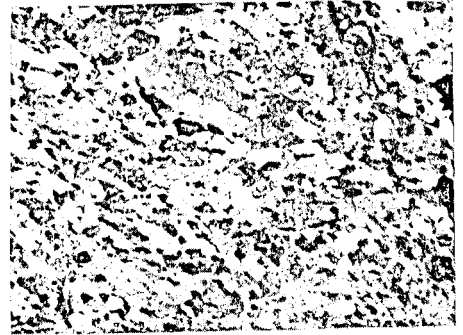
To examine crystallographic texture, pole figures were measured under standard reflection mode and the orientation distribution functions (ODF) were computed using the popLA software package [2]. The volume fractions of several texture components were developed from the ODF.

### Results and Discussion

Subgrain refining with each rolling pass was evident in samples with entry temperatures of 400 and 450° C. Figure 3(a) shows that the microstructure, after the 1st pass at the 450° C entry temperature sample, has subgrain development within each columnar grain. There were pancake-shaped subgrains in some of the grains and equiaxed subgrains in others. The crystallographic orientation of the original as-cast grain must play a role in alignment of the subgrains. Tsuzaki et al[3] reported that the recrystallization kinetics were strongly dependent upon the initial orientations of columnar grains in ferritic stainless steel.



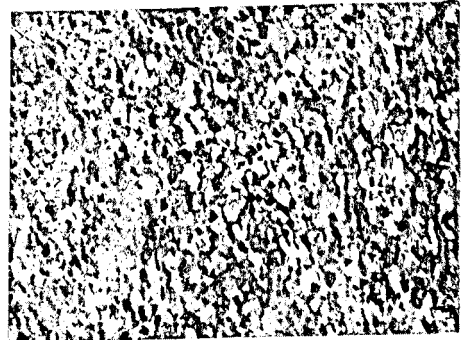
(a)



(b)



(c)

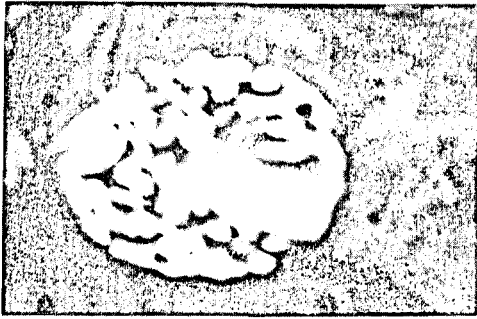


(d)

50  $\mu\text{ms}$

Figure 3: ECC photomicrographs of hot-rolled samples showing subgrain refinement after (a) 1st pass, (b) 2nd pass, (c) 3rd pass and (d) 4th pass.

Although subgrain size was not quantified due to a substantial shape and size variation across the sample, there appeared to be a general refining in sub-grain size as well as a change of shape from pancake to equiaxed (Figures 3(a) through (d)). The grey-level differences in subgrains are due to differences in the crystallographic orientations of the individual subgrains. Dadson & Doherty[4] have reported general refining of subgrains, with increasing amounts of deformation and decreasing deformation temperature in high-purity aluminum alloys. With increasing deformation, the original as-cast grain boundaries were observed to be broken.



1 μm

Figure 4: ECC photomicrograph of hot-rolled samples showing fragmented  $Al_3Fe$  intermetallic rod.

Subgrains did not show any special preference for evolving near as-cast grain boundaries or eutectic particles ( $Al_3Fe$ ).  $Al_3Fe$  intermetallics have been reported[5] to be one of the hardest and were fragmented (Figure 4) possibly due to the large difference in the hardness of matrix vs. particles. In the downstream processing of these bars, intermetallics are broken up further and large particles ( $> 1 \mu m$ ) become sites for nucleation of recrystallized grains and smaller ones ( $\leq 0.1 \mu m$ ) pin the (sub)grain boundaries[6].

A curious phenomenon of sample twisting was observed during the 4th pass and is shown in Figure 5.

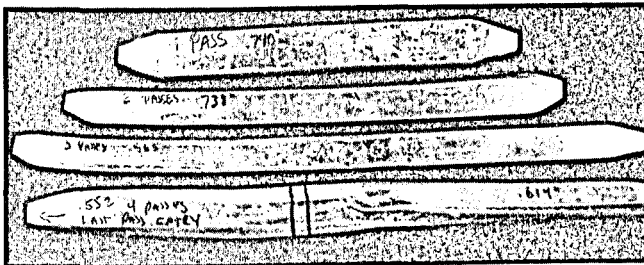
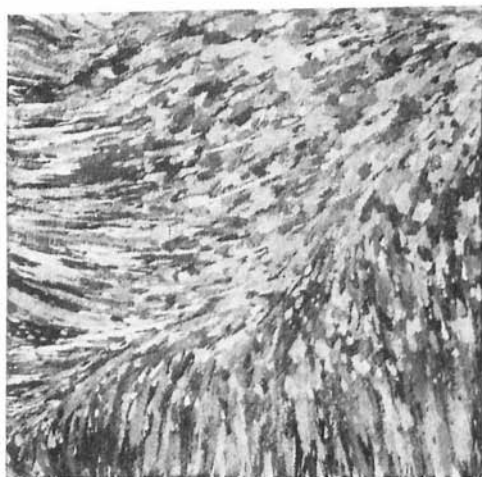
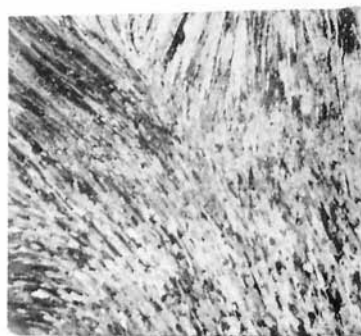


Figure 5: Photomacrograph of hot-rolled samples showing twisting of the rod in the 4th pass.

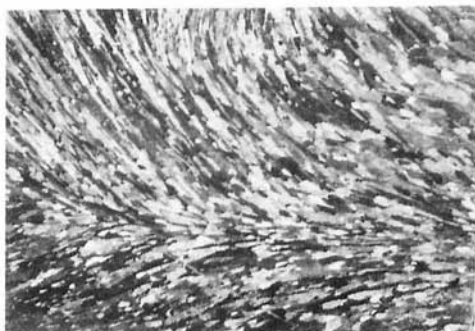
The deformed shape exhibited in the 4th pass resulted from a transverse shearing in the roll bite and was observed for both initial temperatures. The direction of the shearing, or twist of the specimen, was repeatable. Upon a  $90^\circ$  twist of the specimen, the remainder of the bar passed through the bite with little or no reduction. This is due to the similar roll gap setting used for the 3rd and 4th passes. Figures 6(a) through (e) are macrographs of sample cross-sections normal to rolling direction from as-cast to 4th hot-rolling passes, respectively. After the 4th pass the twisting can be seen in Figure 6(e). Figure 6(a) shows the presence of an inhomogeneous arrangement of columnar grains in the as-cast state and "swirled" appearance of grains as the rolling is performed leading to twisting in the 4th pass (Figure 6(e)).



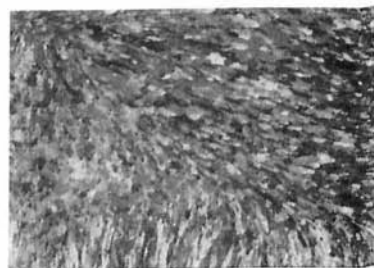
(a) As-cast



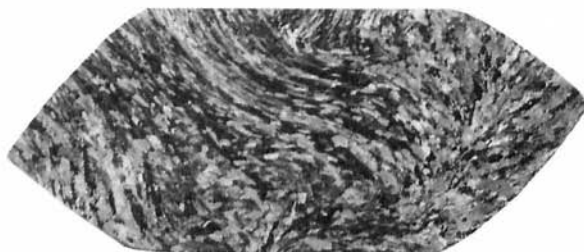
(c) 2nd Pass



(b) 1st Pass



(d) 3rd Pass



(e) 4th Pass

4 mm

Figure 6: Macrographs of hot-rolled samples showing the flow-pattern of grains from (a) as-cast to 4 rolling reductions in (b), (c), (d) and (e) respectively.

The experimental observation of twisting, along with the appearance of regions of shear (seen in the macrograph of Figure 6 (e)), indicate the onset of flow localization. Such localization may follow from crystallographic texture, deformational heating, frictional effects, and tool workpiece heat transfer, all of which are effects in the present experimental regime[7].

Pole figures were measured using a cross-section of the undeformed (after twist) section of a 4th pass specimen and compared to the 3rd pass configuration to establish rolling and normal directions. Quantitative analysis showed  $\{001\}\langle 110 \rangle$  (rotated cube) and  $\{011\}\langle 100 \rangle$  (Goss) to be the dominant crystallographic components, with equivalent volume fractions of each. However, the texture was too weak to be considered as a likely initiator of localization.

The average value of hardness measurements taken from the center of cross-sections of the quenched specimens is plotted in Figure 7. Also shown are the minimum and differential readings from the edges of the specimen in contact with the rolls for the 4th pass (e.g., the transverse edges of the 3rd pass). The general trend displays a saturation of the hardness upon completing the 3rd pass. As there was no evidence of recrystallization in water-quenched samples, the hardness change was deemed indicative of interpass recovery. Inhomogeneity in the as-cast macrostructure (i.e., non-uniform columnar grain distribution) would be expected to contribute to asymmetry in softening.

The edge-to-edge variation in hardness following the 3rd pass corresponds to a likely top-to-bottom variation in flow stress in the 4th pass. With such a condition, establishment of compressive force equilibrium through the approximately rectangular cross-section (Figure 6(d)) will require local gradients in deformation. The result is the shearing in the plane of the cross-section whose normal is the rolling direction. The tendency for shear band formation is commonly observed in plane strain operations[7]. Note that a state of plane strain in the cross-section is supported by the samples shown in Figure 5; the length of the bar does not elongate in the 4th pass.

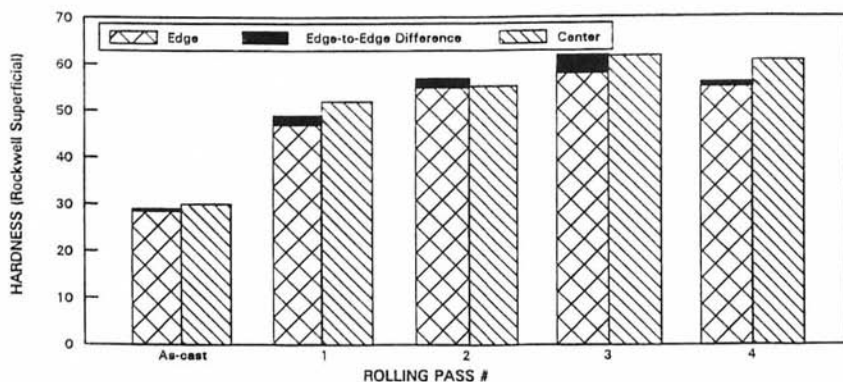


Figure 7: Average hardness measured in the cross-sections perpendicular to the rolling direction in the laboratory hot-rolled rods.

### Conclusions

Channelling contrast mode on SEM was used effectively to reveal the recovered subgrain structure of the hot-deformed samples. Subgrain refinement with increasing hot-rolling reductions was observed. Twisting of sample in the 4th pass was attributed to uneven softening across the sample, resulting in instability. The asymmetrical softening was confirmed by increased edge-to-edge hardness differences in the 3rd pass.

### Acknowledgements

The authors would like to thank Reynolds Metals Company for permission to publish this study. Expert assistance by Timothy Whalen, Lori Showalter, Adrienne Bouldin, Gene Faison, Keith McAllister and Arthur Blackwell is gratefully acknowledged. The authors are also indebted to Carl Necker of Los Alamos National Laboratory for measurement and assistance in the analysis of the pole figures.

### References

1. H. J. McQueen and D. Bourrell, pp. 341-368, Formability and Metallurgical Structure, eds. A. K. Sachdev and J. D. Embury (The Minerals, Metals & Materials Society, 1987).
2. J. S. Kallend, V. F. Kocks, A. D. Rollett and H. R. Wenk, Mat. Sci. and Eng., A123, (1991), 1.
3. K. Tsuzaki, N. Tsuji and T. Maki, pp. 151-156, Recrystallization '90, ed. T. Chandra, (The Minerals, Metals & Materials Society, 1990).
4. A. B. C. Dadson and R. D. Doherty, Acta Metall. 39, (1991), 2589.
5. R. Kovacheva, Prakt. Metallogr. 30, (1993), 2, pp. 68-81.
6. E. Chia and E. A. Starke, Jr., Metall Trans. 8A, (1977), 825.
7. S. L. Semiatin and J. J. Jonas, Formability & Workability of Metals: Plastic Instability & Flow Localization (American Society for Metals, Metals Park, Ohio, 44073, USA, 1984).